



Crash and Flow Analysis of an Super Sonic Aircraft Using Ansys

Mr. L. Bhavani Shankar¹, K. Jaswanth², M. Nithin³, G. Michayelu³, K. Appa Rao³, D. Sravan³, B. Venkat Sai³

^{1,2,3}Avanathi Institute of Engineering and Technology

ABSTRACT

To apply boundary conditions as input, obtain lift and drag coefficient plots, see how streamlines and volume rendering are generated on an aircraft, and then perform explicit dynamics on an aircraft running at various velocities for various materials. Finally, examine how deformation and stresses affect the body. Analyze the aircraft's greatest and minimum deformation as well as its stresses. Information about the state of the aircraft manufacturing industry, the status of aircraft assembly coordination, and development trends. The feasibility of visual and integrated coordinate design, assembly coordination scheme simulation, and knowledge-based feasibility evaluation are all thoroughly investigated.

Keywords: ANSYS, Deformations, Explicit Dynamics, Flow analysis.

1. Introduction

The F-16, often known as the "VIPER," is the most popular, versatile, and successful multi-fighter in the world. In 1976, the F-16 falcon was introduced and sent into service with the USAF. As it is effective in all multirole jet fighter roles, the F-16 is now in service in 25 different nations. It is equipped with AESA technology, allowing the pilot to view. The best perspective of the target region is provided by a comprehensive digital map with adjustable zoom levels. For more than 36 years, Lockheed Martin has been producing the F16 Fighting Falcon. The Lockheed Corporation has a proven track record of creating a variety of high-quality products and parts that can survive all types of weather. The F-16 can carry 3000 pounds (570 liters) more fuel and has an external fuel tank capacity of 600 gallon (2271.25 liters), making it a strategic operational upgraded fighter.



Figure 1. Super Sonic Air Craft

Specifications f-16 falcon

Length	-	49.3 feet/ 15.027meters
Height	-	16.7 feet/ 5.090meters
Speed	-	1500mph (Mach 2+)
Wing span	-	31 feet/ 9.449meters
Empty weight	-	20300lb/ 9207kg
Engine throat class	-	29000lb/ 13000kg

Maximum TOGW	-	48000lb / 21772 kg
Design load faster	-	9g

Literature review

W. Yang, M.N. Hammoudi, G. Herrmann, M. Lowenberg, X. Chen [1] described on "Two-state dynamic gain scheduling control applied to an F16 aircraft model" on September 8, 2012. It is studied if it is feasible and advantageous to use a unique multi-variable dynamic gain scheduling (DGS) method on a sophisticated "industry-scale" aircraft model, which is a non-linear description of the inherently unstable F16 aircraft and includes extensive aerodynamic data. Using a unique control strategy called DGS, controller gains are timed to coincide with one (or more) of the system states while taking into consideration the "hidden coupling terms" to guarantee a nearly optimal response. It works well for non-linear systems that vary rapidly between operational points.

Gwang-gyoSeo, Yoonsoo Kim, SubrahmanyamSaderla, On April 7, 2019, "Kalman-filter based online system detection of fixed-wing aircraft in upset condition" was assessed. Online system identification has grown in importance as a result of technological advancements in the development of techniques for calculating aerodynamic parameters. This research suggests two online system identification (SID) techniques based on Kalman filters to estimate the aerodynamic properties of fixed-wing aircraft in unstable situations like stalls.

Ghazala Akram, Maasoomah Sadaf 2016 In order to solve ninth order boundary value problems in AFTI-F16 fighters, homotopy analysis approach is applied. The ninth order boundary value difficulties that arise in the mathematical modeling of the AFTI-F16 fighter are the focus of this essay. The ninth order differential equations that describe the AFTI-F16 fighter's enhanced longitudinal and lateral dynamics contain unknown parameters that can be found utilizing automated system identification procedures. With the homotopy analysis approach, the boundary value issue is solved in terms of a convergent series (HAM). The approach is successfully used on numerical instances, and when the outcomes are compared to those reported in the literature, it becomes clear that the proposed approach provides superior approximations to the precise answer.

James C. Williams, Edgar A. Starke, Jr. 2003 "Progress in structural materials for aircraft systems" was discussed. The development of aircraft and aviation engines is examined in this study in terms of the contribution that improved materials and technology have made. This development covers the relatively recent shift in the aircraft industry from producing just goods driven by performance to producing products driven by consumer value. It is shown that most of the advancement since the invention of human, heavier-than-air flight has been made possible by developments in materials, processing technologies, and knowledge. The introduction of novel materials has altered as a result of current cost restraints, which are defined by consumer value. These changes seem to represent the new paradigm for the aircraft and aircraft engine industries. The function of materials in producing lightweight structures is the larger topic, even if the focus of this study is on aero planes and aviation engines. Once they have been cost-adjusted, several of the examples given in this study are applicable to automotive applications.

Jacek Pieniasek 2019 "Aircraft approach measurement using airfield picture" The most dangerous part of the trip is as the plane approaches the runway. To ensure appropriate flight control and control decision-making, it is essential to measure the aircraft's location in respect to the runway. Although there are many measuring techniques in use in aviation, human pilots in VFR circumstances utilize views of the airport to determine the location of their aircraft. The foundation for a new measuring approach is an airfield picture and details about the actual locations of markers in the runway coordinate frame. After localizing markers, such as present airport features and runway paintwork, the position of the aero plane is calculated by resolving equations expressing geometric connections. The algorithm, analysis of measurement accuracy, and examples of the outcomes of in-flight experiments are described in this paper. In order to suggest camera system parameters, the study takes into account a number of variables, including camera resolution, marker size, and aircraft position.

3. Modeling and Methodology

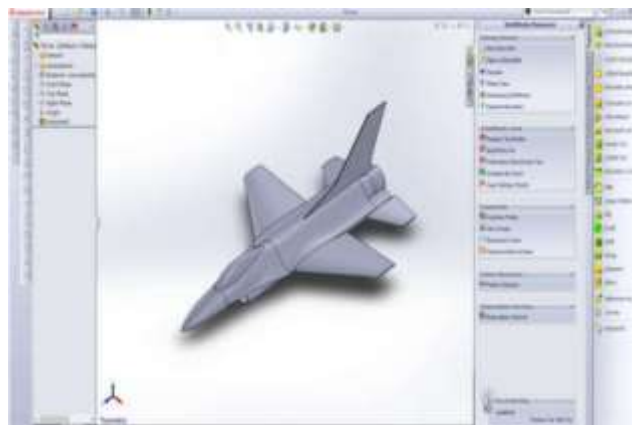


Figure 2. Solid Works Model

Imported Model into ANSYS

The ANSYS workbench receives an imported model created in Solid Works. This is a display of the imported geometry.

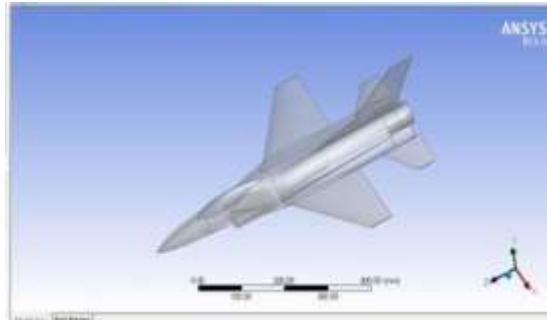


Figure 3. ANSYS Model

Meshing

Meshing is one of the key components of ANSYS, and the body has to be properly meshed for usage in the future. We have flaws in the analytical portion and computations because of the meshing failure.

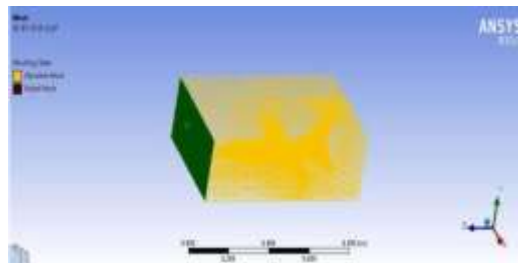


Figure 4. Meshing

Set up the methodology

Setting up the solutions requires providing the relevant inputs, such as gravity, the k-epsilon model, checking the material chosen, and velocity (350 m/s) as the input. Reference values are then provided, the computation is conducted, and the velocity streamlines and volume renderings are obtained.

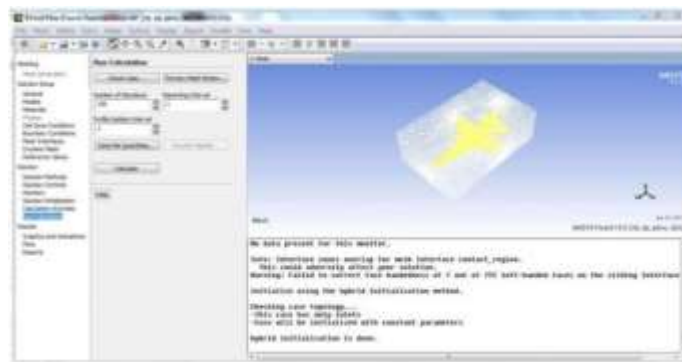


Figure 5. Set Up

ANALYSIS ON F-16

Velocity Streamlines:

The concept of streamlines is crucial to the study of aerodynamics. The route that a mass-less particle follows as it goes with the flow is known as a streamline. The illustration below demonstrates how 350 m/s velocity streamlines hit the solid F-16 model.

The blue stream lines which impact on the body will not affect the body of the aircraft. The yellow streamlines impacts on the body will affect the body.

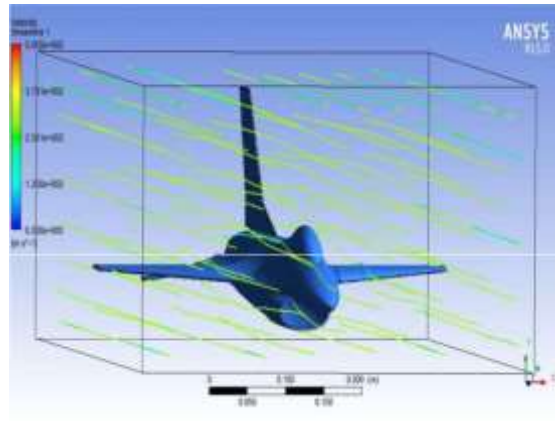


Figure 6. Velocity Streamlines

Explicit Dynamics:

Imported model from SOLIDWORKS into ANSYS

The model which is done in SOLIDWORKS is imported into ANSYS

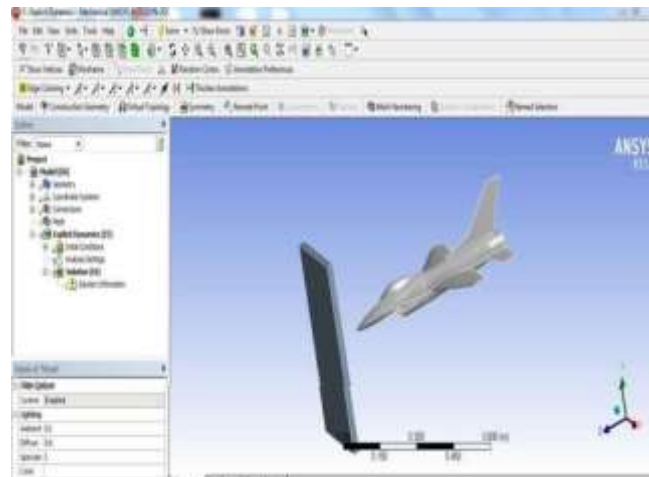


Figure 7. Imported model in the ANSYS

Generating of mesh:

Meshing should be done for the solid model without any errors. The F-16 model contains 6399 nodes and 21933 elements.

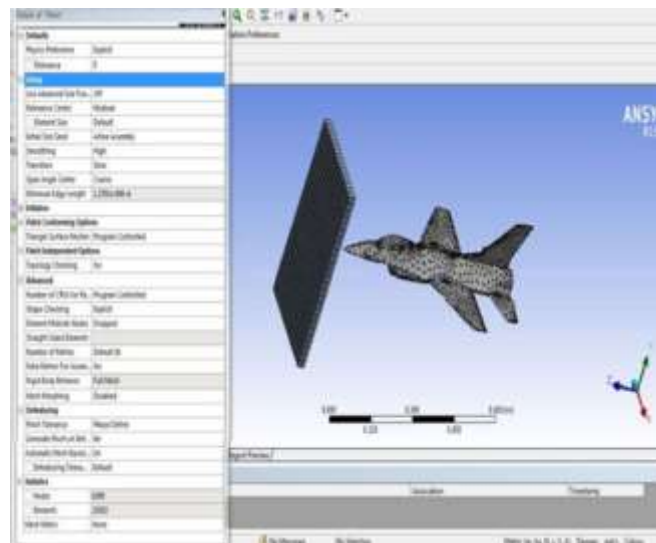


Figure 8. Meshing

3.1 For Aluminum Alloy

The figures below, numbered 9 to 22, show the total deformation and equivalent stress for aluminum alloy from 300 m/s to 600 m/s. This diagram illustrates how the deformation and stress, which fluctuate with velocity, affect the aircraft's body.

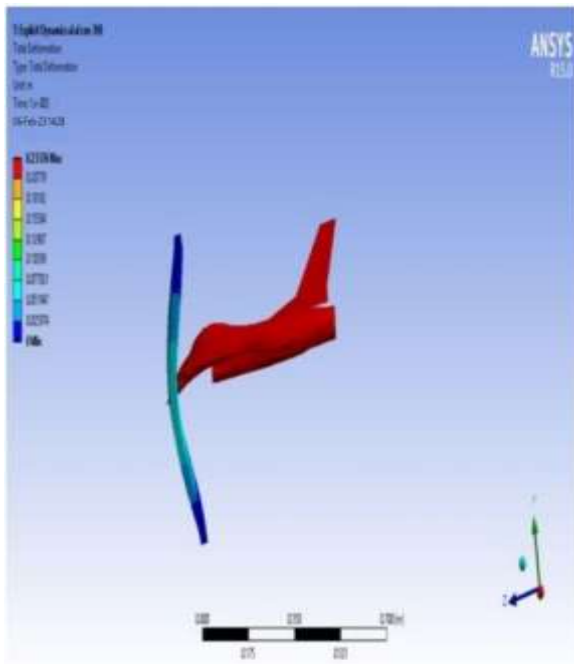


Figure 9. Deformation at a velocity 300m/s

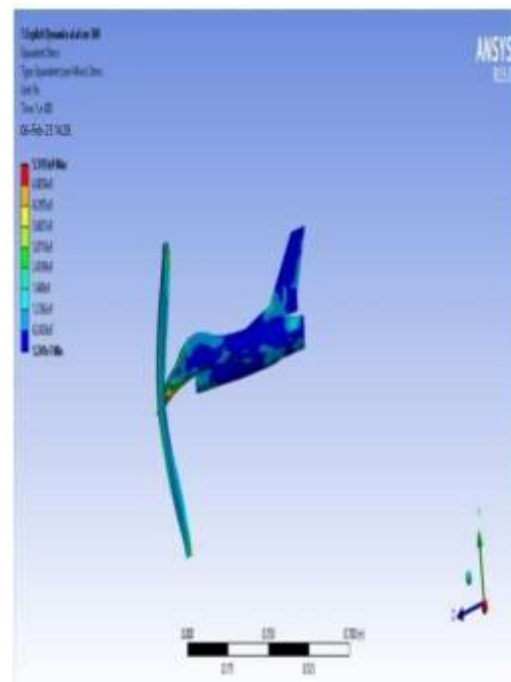


Figure 10. Stresses at a velocity 300m/s

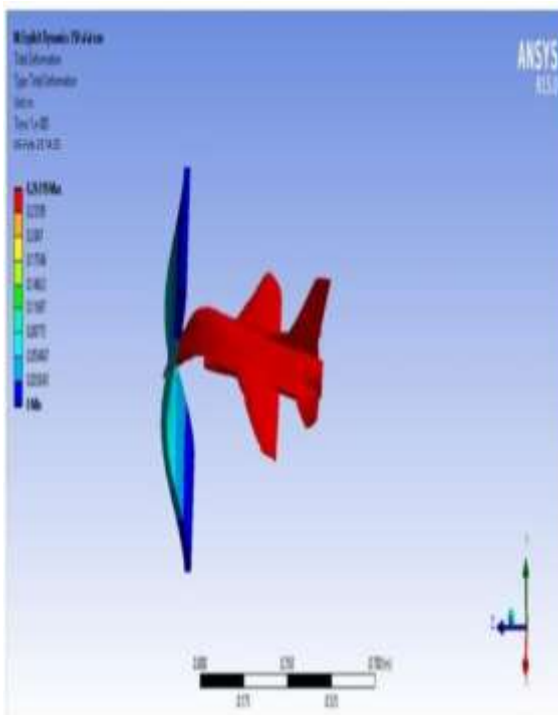


Figure 11. Deformation at a velocity 350m/s

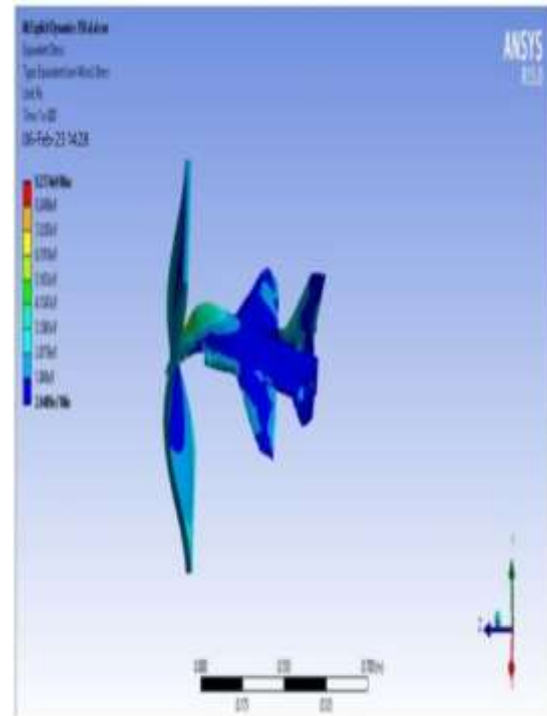


Figure 12. Stresses at a velocity 350m/s

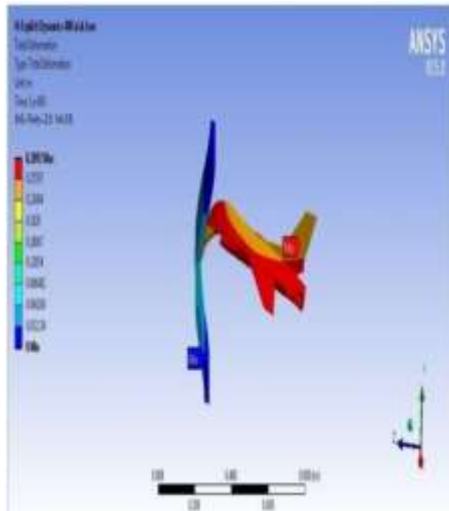


Figure 13. Deformation at a velocity 400m/s

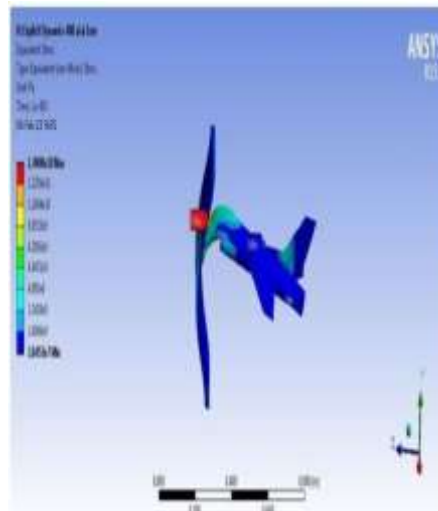


Figure 14. Stresses at a velocity 400m/s

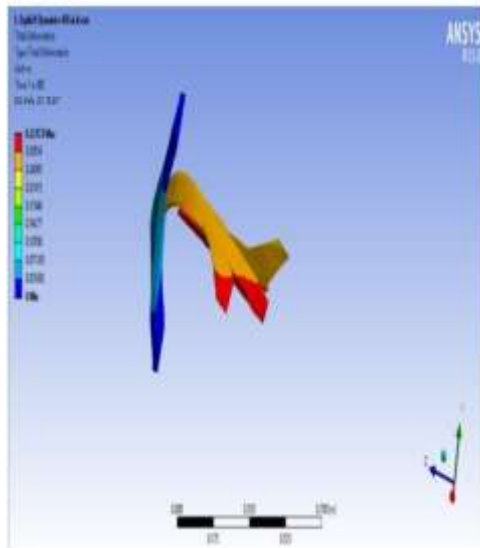


Figure 15. Deformation at a velocity 450m/s

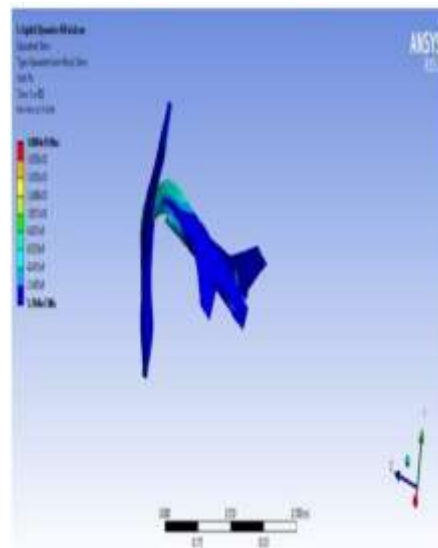


Figure 16. Stresses at a velocity 450m/s

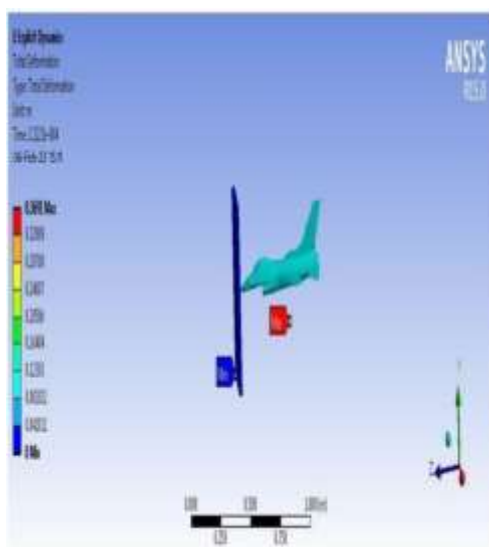


Figure 17. Deformation at a velocity 500m/s

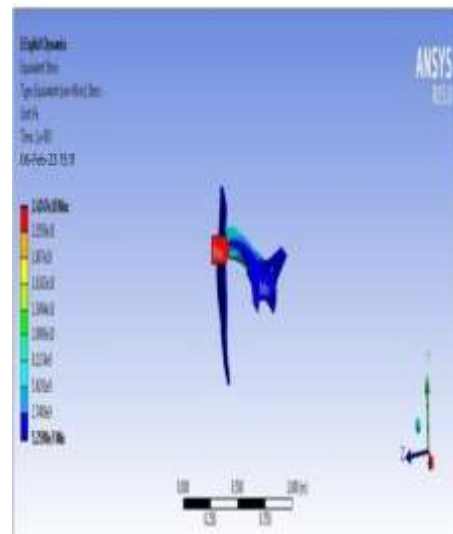


Figure 18. Stresses at a velocity 500m/s

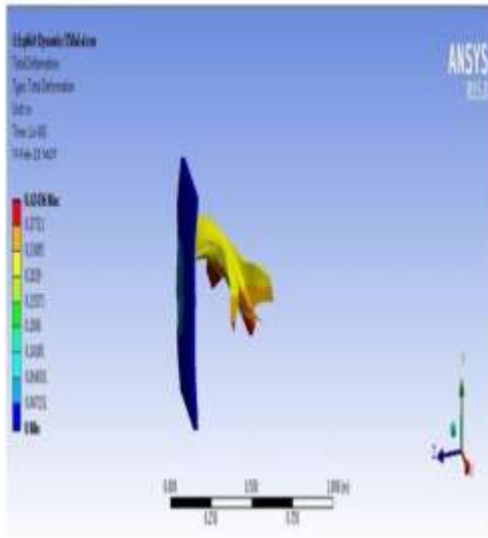


Figure 19. Deformation at a velocity 550m/s

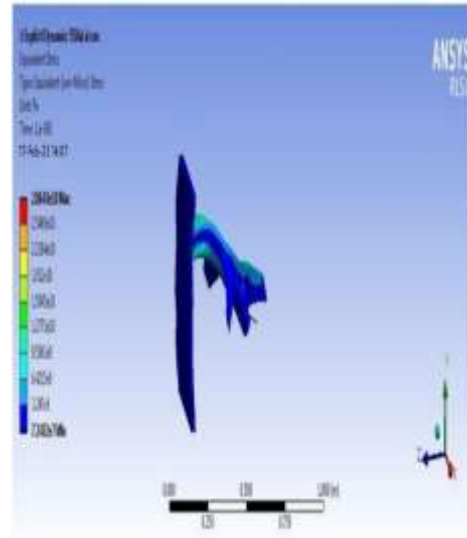


Figure 20. Stresses at a velocity 550m/s

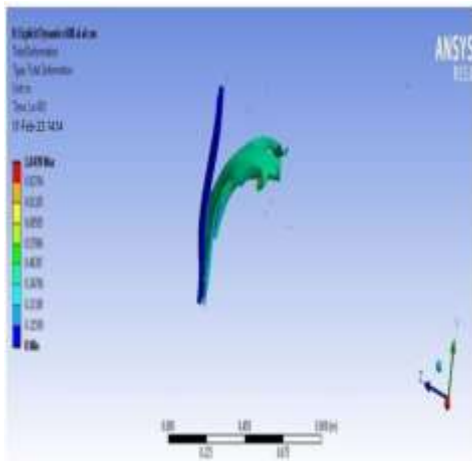


Figure 21. Deformation at a velocity 600m/s

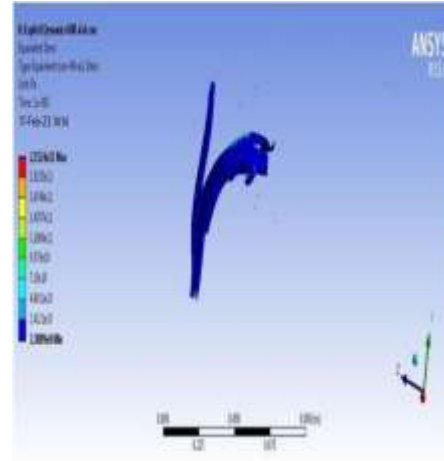


Figure 22. Stresses at a velocity 600m/s

3.2 For Stainless Steel

The figures below, numbered 23 to 36, show the total deformation and equivalent stress for stainless steel at velocities ranging from 300 m/s to 600 m/s. This diagram illustrates how the deformation and stress, which fluctuate with velocity, affect the aircraft's body.

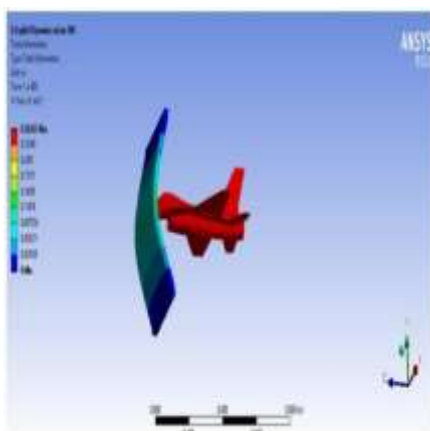


Figure 23. Deformation at a velocity 300m/s

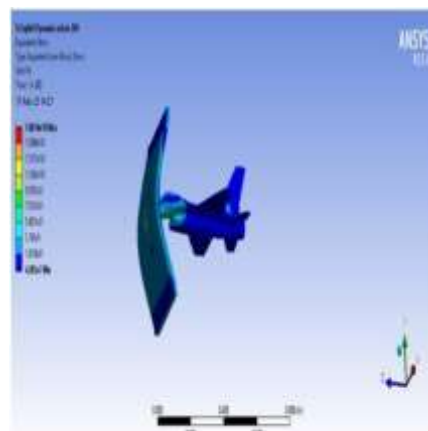


Figure 24. Stresses at a velocity 300m/s

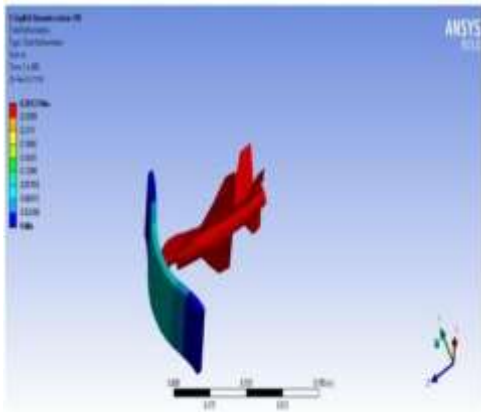


Figure 25. Deformation at a velocity 350m/s

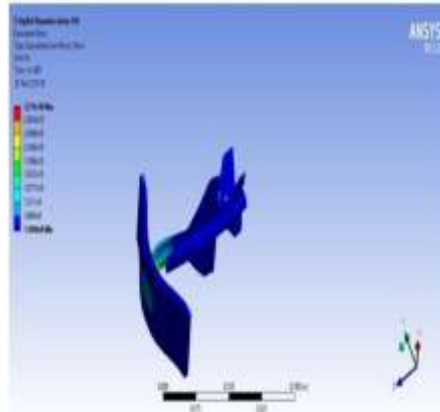


Figure 26. Stresses at a velocity 350m/s

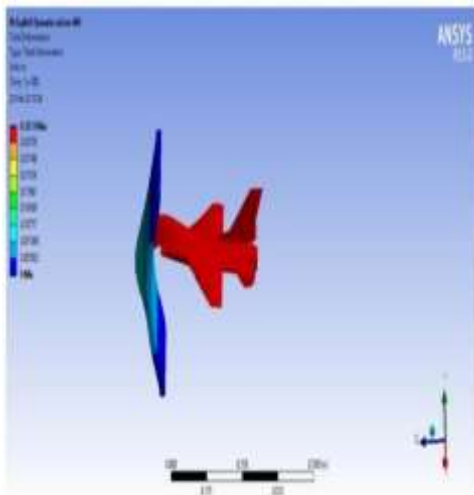


Figure 27. Deformation at a velocity 400m/s

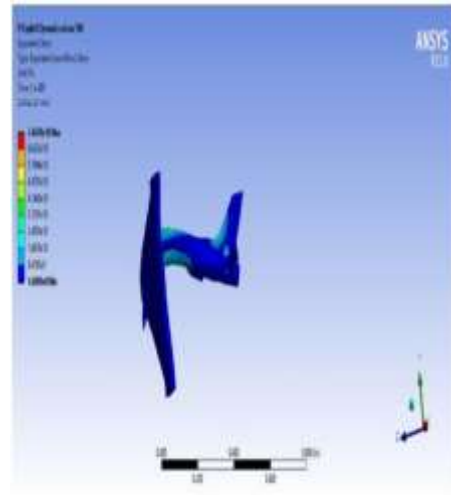


Figure 28. Stresses at a velocity 400m/s

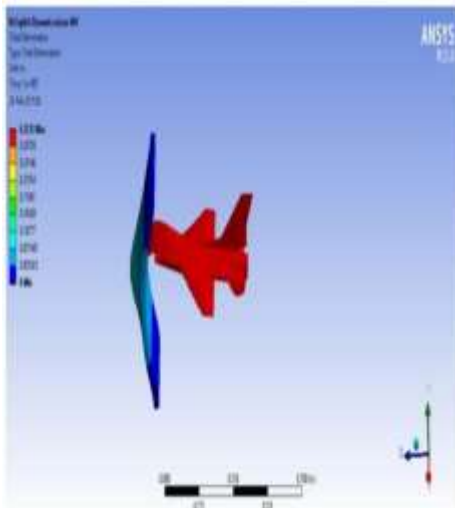


Figure 29. Deformation at a velocity 450m/s

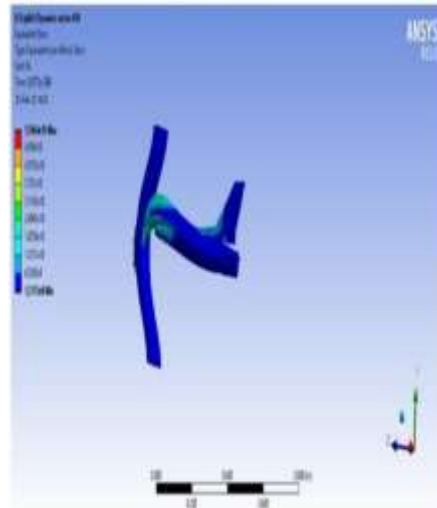


Figure 30. Stresses at a velocity 450m/s

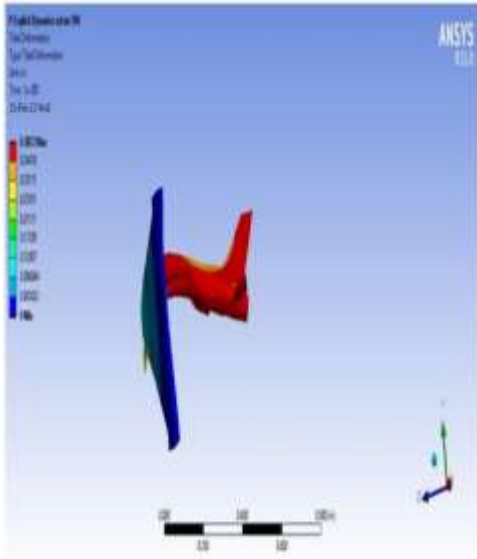


Figure 31. Deformation at a velocity 500m/s

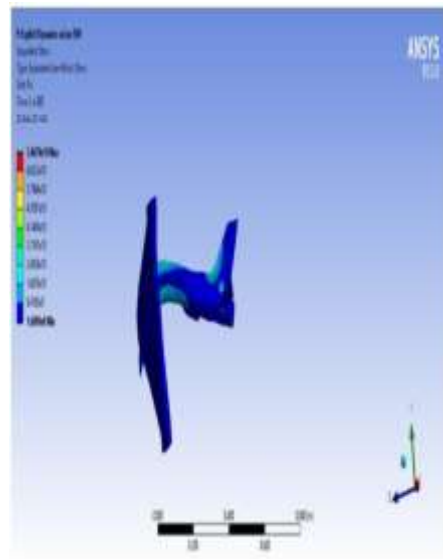


Figure 32. Stresses at a velocity 500m/s

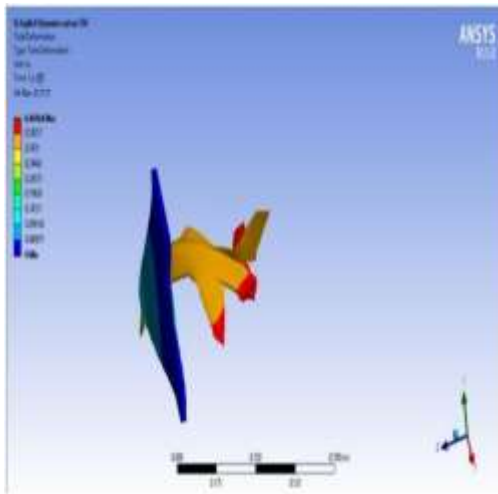


Figure 33. Deformation at a velocity 550m/s

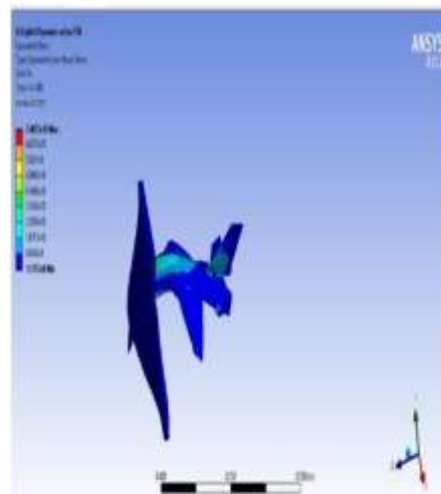


Figure 34. Stresses at a velocity 550m/s

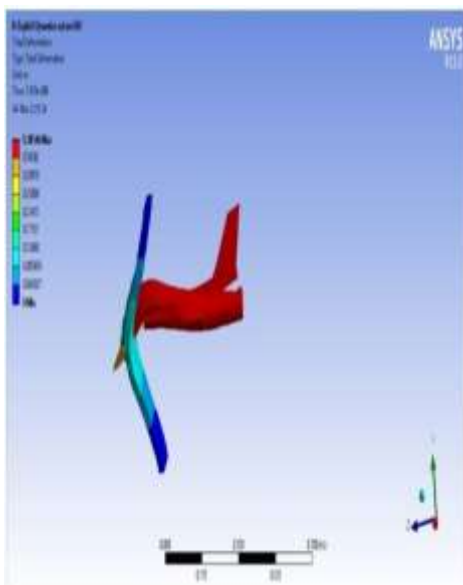


Figure 33. Deformation at a velocity 600m/s

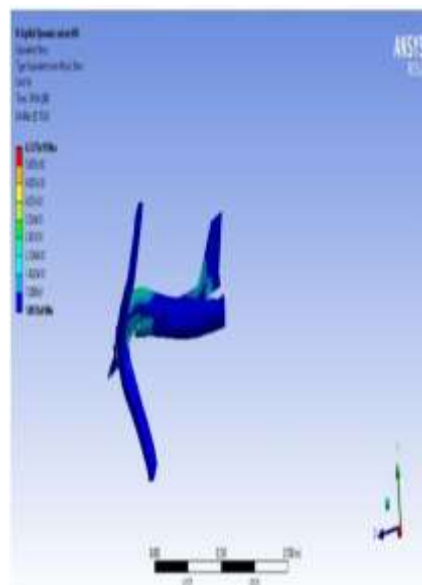


Figure 34. Stresses at a velocity 600m/s

4. Results and Discussions

The maximum deformation and maximum stress for an aluminum alloy at various speeds are shown in table.1. We may infer from the table that an increase in velocity will result in an increase in stress and deformation of the aircraft's body. Maximum stress increases from 300 m/s to 350 m/s and, in the case of aluminum alloy, from 400 m/s to 600 m/s velocity. Higher velocities cause the body to deform more dramatically, which causes the model to fail.

Table.2 displays the maximum deformation and maximum stress for stainless steel at various speeds. We may infer from the table that an increase in velocity will result in an increase in stress and deformation of the aircraft's body. Higher velocities cause the body to deform more dramatically, which causes the model to fail.

By the comparison between the two materials the aluminum alloy is best suited material for the manufacturing the aircraft.

The graphs are shown for velocity (m/s) on the X-axis vs. deformation (m) on the Y-axis in figure 37 and velocity (m/s) on the X-axis vs. maximum stress (pa) on the Y-axis in figure 38. In both figures, the deformation and maximum stress are shown for the aluminum alloy in blue and the stainless steel in orange, respectively.

Table. 1 aluminum Alloy

Velocity (m/s)	Maximum Deformation (m)	Maximum Stress (pa)
300	0.23376	8.68e ⁰⁰⁹
350	0.24056	7.033e ⁰¹⁰
400	0.2892	1.4908e ⁰¹⁰
450	0.32123	1.8884e ⁰¹⁰
500	0.3691	2.4247e ⁰¹⁰
550	0.42436	2.8643e ⁰¹⁰
600	1.0439	2.6917e ⁰¹¹

Table. 2 Stainless Steel

Velocity (m/s)	Maximum Deformation (m)	Maximum Stress (pa)
300	0.26267	1.6983e ⁰¹⁰
350	0.29237	3.211e ⁰¹⁰
400	0.3233	4.6527e ⁰¹⁰
450	0.33613	5.5964e ⁰¹⁰
500	0.3872	7.9307e ⁰¹⁰
550	0.44164	8.6133e ⁰¹⁰
600	1.38544	6.3371e ⁰¹⁰

Fig. 35. Deformation (m) Vs. Velocity (m/s)

Fig. 36. Maximum Stress (pa) Vs. Velocity (m/s)

5. CONCLUSION

- It is observed that, for the both materials has the velocities increases deformation and stresses also increases.
- Maximum stress is increasing from 300m/s to 350m/s velocities and from 400 to 550 m/s velocity in case, of aluminium alloy.
- Aluminium alloy is suitable for F-16 aircraft because it is having less with when compared to stainless steel.
- Aluminium alloy is having less deformation and stress when compared to stainless from 300m/s to 550m/s.

References

- [1] **BabithaKodavanla, Dr P K Dash, Dr P Srinivas Rao**, "Computational Aerodynamic Analysis of F-16 Falcon Wing" Institute of Aeronautical Engineering, Dundigal, Hyderabad, India. Volume 4, Issue 11, November 2017.

-
- [2] **Mushfiqul Alam, Martin Hromcik**, “Structural load alleviation using distributed delay shaper Application to flexible aircraft” The University of Liverpool, School of Engineering, Liverpool, United Kingdom, 3 June 2019.
- [3] **W. Yang, M.N. Hammoudi, G. Herrmann, M. Lowenberg, X. Chen**, “Two-state dynamic gain scheduling control applied to an F16 aircraft model” College of Aerospace and Materials Engineering, National University of Defense Technology, Changsha, Hunan 410073, PR China, Department of Aerospace Engineering, University of Bristol, Bristol, BS81TR, UK, Department of Mechanical Engineering, University of Bristol, Bristol, BS81TR, UK. 8th September 2012.
- [4] **Gwang-gyo Seo, Yoonsoo Kim, Subrahmanyam Saderla**, “Kalman-Filter Based Online System Identification Of Fixed-Wing Aircraft In Upset Condition” Graduate School of Mechanical and Aerospace Engineering and ReCAPT, Gyeongsang National University, Jinju 52828, Republic of Korea, Department of Aerospace Engineering, Indian Institute of Technology Kanpur, Kanpur, India 7th April 2019.
- [5] **Aircraft Abhilash P. M, Niranjana K. Sura, Vijay V. Patel, Girish S. Deodhare**, “Development and flight test on an Automatic Leveling Function for a Fighter” Integrated Flight Control Systems, Aeronautical Development Agency, Bangalore – 560017, India (Tel: 080-2508-6535).
- [6] **Antony Jameson, Kui Ou**, “50 years of transonic aircraft design” Aeronautics and Astronautics Department, Stanford University, United States. 9th February 2011.
- [7] **Gregson, P. J.**, discussed on “Aluminium alloys for Aircraft Structures” In High performance materials in aerospace, ed. H. M. Flower, Chapman & Hall, London, 1195, pp. 49–83.
- [8] **Ghazala Akram, Maasoomah Sadaf**, “Application of Homotopy Analysis Method to the Solution of Ninth Order Boundary Value Problems in AFTI-F16 Fighters”, Department of Mathematics, University of the Punjab, Lahore 54590, Pakistan 2006.
- [9] **James C. Williams, Edgar A. Starke, Jr.**, A Materials Science & Engineering Department, The Ohio State University, 142 Hitchcock Hall, 2070 Neil Ave, Columbus, OH 43210, USA b Materials Science & Engineering Department, The University of Virginia, Thornton Hall, Room B102A, Charlottesville, VA 22903, USA 2003.
- [10] **M. Sujataa, M. Madana, K. Raghavendraa, N. Jagannathanb, S.K. Bhaumika**, “Unraveling the cause of an aircraft accident” A Materials Science Division, Council of Scientific & Industrial Research (CSIR), Bangalore 560017, India. Structural Technologies Division, National Aerospace Laboratories, Council of Scientific & Industrial Research (CSIR), Bangalore 560017, India.
- [11] **Eirikur Jonsson, Cristina Riso, Christopher A. Lupp, Carlos E. S. Cesnik, Joaquim, R. R. A. Martins, Bogdan I. Epureanu** “Flutter and Post-Flutter Constraints in Aircraft Design Optimization”, Department of Aerospace Engineering, University of Michigan, Ann Arbor, MI, 48109, USA, 31 May 2019.
- [12] **Jacek Pieniazek** Dept. of Avionics and Control, Faculty of Mechanical Engineering and Aeronautics Rzeszow University of Technology Rzeszow, Poland 26 March 2019.
- [13] **Zheng Penga, Wang Junliangb, Zhang Jie, Yang Changqic, Jin Yongqiaoc**. “An Adaptive CGAN/IRF-Based Rescheduling Strategy for Aircraft Parts Remanufacturing System Under Dynamic Environment” School of Mechanical Engineering, Shanghai Jiao Tong University, Shanghai 200040, China. College of Mechanical Engineering, Donghua University, Shanghai 201620, China Shanghai Spaceflight Precision Machinery Institute, Shanghai 201699, China. March 2019.
- [14] **Dongping Zhao, Gangfeng Wang, Wen Guo, Qi Zhang** “An Integrated Framework for Aircraft Digital Assembly Coordination Design and Simulation” school of aircraft engineering, Xi’an Aeronautical University, Xi’an 710077, China